

Binary Stochastic Filtering: a Solution for Supervised Feature Selection and Neural Network Shape Optimization

A. Trelin^{a,*}, A. Procházka^b

^a*Department of Solid State Engineering, University of Chemistry and Technology, 16628 Prague, Czech Republic*

^b*Department of Computing and Control Engineering, University of Chemistry and Technology, 16628 Prague, Czech Republic*

Abstract

Binary Stochastic Filtering (BSF), the algorithm for feature selection and neuron pruning is proposed in this work. Filtering layer stochastically passes or filters out features based on individual weights, which are tuned during neural network training process. By placing BSF after the neural network input, the filtering of input features is performed, i.e. feature selection. More than 5-fold dimensionality decrease was achieved in the experiments. Placing BSF layer in between hidden layers allows filtering of neuron outputs and could be used for neuron pruning. Up to 34-fold decrease in the number of weights in the network was reached, which corresponds to the significant increase of performance, that is especially important for mobile and embedded applications.

Keywords: Feature selection, dimensionality reduction, neural network, neuron pruning

*Corresponding author

Email address: trelina@vscht.cz (A. Trelin)

Preprint submitted to Applied Soft Computing

February 13, 2019

1. Introduction

Majority of machine learning algorithms rely on pre-selected datasets for training and further prediction. There is a variety of cases where dataset consists of a significant number of different features (e.g. versatile statistical measures for text or network data processing), with only some of them actually bearing information useful for solving given problem (usually classification or regression). The process of finding an information-rich subset is called feature selection, and is of growing interest with the modern development of machine learning. Correct feature selection aims reducing of computational complexity, generalization enhance [1] or may be of interest on its own for further interpretation.

Numerous approaches were proposed in the last 25 years (Fig. 1), which include algorithms based on information theory, that tries to estimate the amount of information, brought to the dataset by a given feature [3, 4, 5], Relief and derived algorithms [6, 7], based on nearest neighbor search, statistical [8] and spectral graph theory based [9], etc. The very modern approaches are mainly focused on application of swarm intelligence algorithms [10, 11, 12] Unfortunately, different methods usually lead to strongly discrepant sets of features, and final decision could be made only after series of experiments.

This paper proposes a feature selection method which rely on the intrinsic optimization algorithms, used in machine learning without any external modification. The filter layer is directly introduced into the neural network (NN), being trained by the standard backpropagation, leading to increase of important features weights. In addition, filtering may be utilized for neuron pruning, which could lead to multifold increase of NN performance.

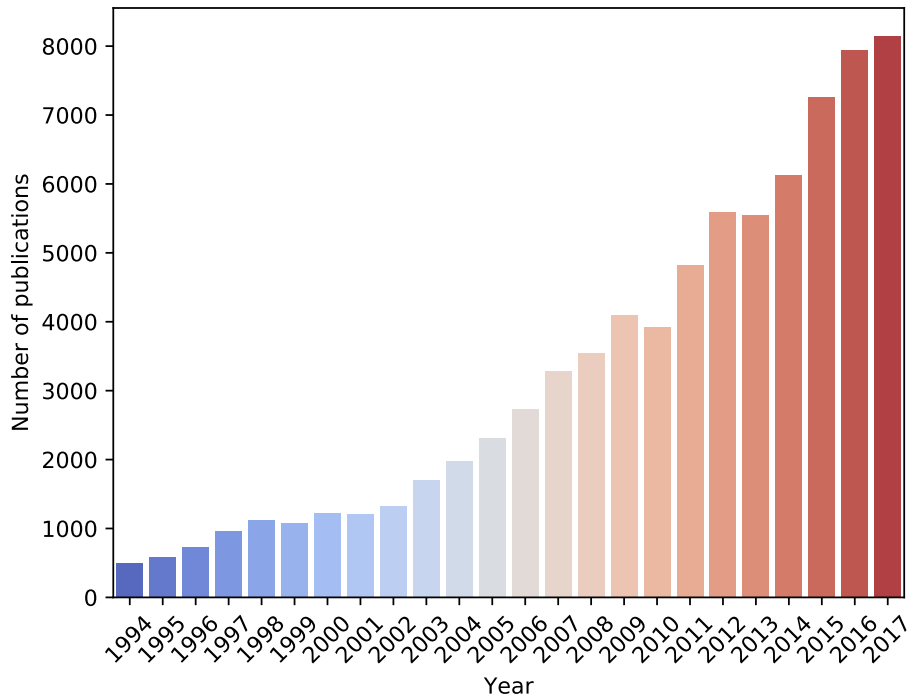


Fig. 1: Number of publications considering feature selection in past years. Image is generated based on data from the Web of Science service [2], searched for topic: “feature selection”.

The method can be applied to different kinds of NN, optimized for various datasets, which will be demonstrated in this work.

2. Method

Stochastic neurons, the units with nondeterministic behavior are known for a long time, at least since mid 1980s, when Boltzmann machines became popular [13]. In addition, the stochastic neurons are of interest because of their closeness to the biological ones [14]. A successful networks, consisting of stochastic neurons were built [15]. Nevertheless, mixing of stochastic

and deterministic units in one network is not popular subject, except for Dropout technique [16], which works by randomly disabling deterministic neurons in order to prevent overfitting.

Proposed algorithm is inspired by both stochastic neurons and dropout. The method basically combines two above-mentioned ideas and could be thought as generalization of dropout with trainable individual dropout rates or as incorporation of special version of stochastic neurons into classical deep NN structure. Proposed binary stochastic filtering (BSF) method works by setting the BSF layer (consisting of the BSF units) after the layer, outputs of which is to be filtered. BSF unit stochastically passes the input without changes, or sets it to zero with probabilities based on the unit weights. Strictly speaking, BSF unit is described as:

$$BSF(x, w, z) = x_{z < w} \tag{1}$$

where w represents the adjustable weight of a given unit, and z is uniformly sampled from the range $[0, 1]$. This definition is inspired by the formula from the work of Bengio et al. ([17], Eq. (3)). Authors have defined the Stochastic Binary Neuron as $h_i = f(a_i, z_i) = 1_{z_i > \text{sigm}(a_i)}$, where neuron activation a_i is given as a weighted sum of its inputs. This definition is directly derived from the classical deterministic neurons, and utilized as a noisy modification of them. At the same time, binary stochastic filtering unit makes use of the same idea of feeding random uniform noise into the neuron, but input value does not influence the unit output. BSF includes the single input which passes through the unit if random value z is smaller than weight w or nullified instead. Thus, probability of output to be x is equal to the probability of z to be less than w , $\mathbb{P}(x) = \mathbb{P}(z < w)$, which

is equal to $F_z(w)$, where F_z is a cumulative distribution function for the variable z . From the properties of uniform distribution,

$$F_z(w) = \begin{cases} 0, & \text{for } w < 0 \\ \frac{w-a}{b-a}, & \text{for } w \in [a, b) \\ 1, & \text{for } w \geq b \end{cases} \quad (2)$$

on the interval $[a, b]$ from which z is sampled, $F_z(w) = w$, as $[a, b] = [0, 1]$. This allows selective filtering of the layer inputs with adjustable probabilities of the given input to be filtered, which equals the weight w , supposing $w \in [a, b]$. Setting w to be close to 0 means that the given feature is close to be completely filtered out, while in case of w being close to 1, feature passes through BSF without changes. Thereby, by tuning the BSF layer weights it is possible to control how much each of the features participates in the training process.

From the obvious reasons, gradient of a stochastic unit is stochastic as well, being equal to zero or ∞ randomly. Thus, backpropagation training, being a variation of gradient descent method is not able to optimize weights of the BSF units. G. E. Hinton has suggested a straight through (ST) estimator [18], which defines the gradient of stochastic unit with respect to its input $\frac{\partial BSF(x)}{\partial x} = 1$. Few modifications of this approach were reported, such as multiplication of the gradient by a logistic sigmoid derivative, i.e. $\frac{\partial BSF(x)}{\partial x} = \frac{d\sigma(x)}{dx}$, where $\sigma(x) = \frac{1}{1+e^{-x}}$ but it was found that simpler unity gradient achieves better performance [17]. ST estimator is especially suitable when stochastic neurons are mixed with normal ones, as it does not distort the gradient between classical units. Proof of the last statement is given in Appendix A.

Hereby, by applying the ST estimator, weights of BSF layers could be optimized during model training. Moreover, penalizing of the filter weights will lead to decrease of above-lying layer involvement in the NN working process, which could be used for neuron pruning or overfitting prevention. Placing the penalized BSF layer as input layer of the NN, will decrease probabilities of feature occurring in correspondence to their importance, which is equivalent to the feature selection.

2.1. Feature selection

2.1.1. Deep NN classifier

Classifier is a model, performing mapping from n -dimensional data space $D^n \rightarrow L$ to the label space consisting of finite (and usually relatively low) number of labels. As a deep NN classifier, classical multilayer perceptron model with softmax activation of the output layer was used [19]. Softmax function is a generalization of logistic function for a multilabel classification problem, defined as

$$\sigma(\vec{x})_i = \frac{e^{x_i}}{\sum_{j=1}^N e^{x_j}} \quad (3)$$

for $i = 1, 2, \dots, N$ where N describes number of classes in a given problem. Unlike classical binary logistic regression, which outputs the scalar probability p of a data to be true and $1 - p$ to be false, softmax function outputs a vector \vec{p} with length N , each element of which represents probability of the input sample to belong to each of the classes. Normalization by the sum of outputs guarantees that total probability of a sample to belong to all classes will always be unit. Exploitation of the softmax function needs

label to be one hot encoded, i.e. to the vector with length N

$$L_{oh}(i) = \begin{cases} 1, & \text{if } i = \text{classindex} \\ 0, & \text{elsewhere} \end{cases} \quad (4)$$

In that case loss function must describe divergence between \vec{p} and encoded label $L_{oh}^{\vec{}}$, i.e. map two vectors to a scalar. It is a known fact that cross-entropy is an efficient way to describe the error in that case [20]. This function is defined as

$$E = - \sum_{i=1}^N c_i \cdot \ln(p_i) + (1 - c_i) \cdot \ln(1 - p_i) \quad (5)$$

where c_i is the actual class label and p_i is corresponding element of \vec{p} . This function is considered to be the most suited loss for a probabilistic NN classifier [20]. The selected NN model consists of 4 layers with rectified linear activation [21] in the hidden layers. Number of units in each layer was empirically chosen as $D, 2D, D, N$ respectively, where D is the dimensionality of input data, in order to meet the different number of features in used datasets. Model was optimized using Adam algorithm [22] with parameters $\alpha = 0.001, \beta_1 = 0.9, \beta_2 = 0.999$, as it is specified in the original paper with zero learning rate decay. The same optimizer was used for training of all other models.

Classification accuracy for every dataset was estimated using 10-fold cross-validation method. The NN was trained until full convergence was reached (no loss decrease) and both training and testing mean accuracies were used for evaluation of model performance.

Binary stochastic filter was placed as an input layer to the NN of the same structure as classifier, resulting in 5 layer network. L_1 regularization was used as a penalty, with the regularization coefficient defining the

tendency of the data to be filtered out. Generally, coefficient serves as a metaparameter in the filtering layer, and need to be adjusted to meet the classifier loss. Good results were achieved with regularization coefficient lying in the range 0.001-0.01. The examples of training process visualization depending on regularization rate are shown in the supplementary materials. Model was trained until convergence. After model fitting, weights of a BSF layer were analyzed and treated as a feature importances. For selection the highest importance features were manually selected and saved forming a reduced dataset. Afterwards, normal classifier was trained as described above for estimation of classification accuracy for the reduced dataset. To estimate changes in high-dimensional cluster separation, the well known silhouettes method [23] was used. In brief, the method defines silhouette $s(i)$ which compares mean inter-cluster distance $a(i)$ for the given data point i and mean distance to all objects belonging to the nearest cluster $b(i)$.

$$s(i) = \frac{b(i) - a(i)}{\max\{a(i), b(i)\}} \quad (6)$$

The mean value of silhouettes (silhouette coefficient) for all the data-points within dataset is a measure for cluster separation, lying in the range $[-1, 1]$ where higher number means better separation.

2.1.2. Image recognition

Convolutional NN (CNN) makes use of data spatial independence, which is especially useful in image recognition. The CNN architecture was proposed by Le Cun et al. [24] for number recognition problem. Generally, architecture implements discrete convolution operation, which converts input data (image) to the map of features. Convolution kernel is optimized during training process to minimize the loss function. Produced maps of

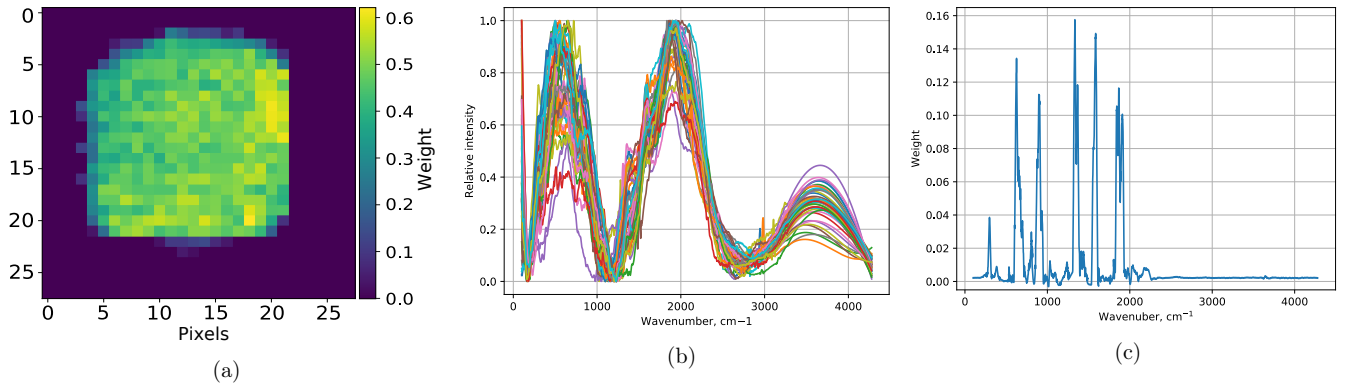


Fig. 2: (a) Weights of the BSF layer after fitting MNIST dataset. (b) Set of Raman spectra of different classes after normalization. (c) Regions of interest of the spectra selected by BSF.

features are convoluted again with larger kernel, leading to higher-order maps. After few subsequent convolution layers the classical fully-connected classifier (described in previous part) is placed, which is able to extract from the maps information about belonging to class [25].

The CNN classifier with structure, described in the Table B.5, was implemented. Its architecture is inspired by the LeNet-5 [25]. In addition to original LeNet, batch normalization was applied to the output of every convolutional layer, which is reported to increase the convergence rate [26]. First 6 layers form the convolutional model, which performs feature extraction from images, while 4 last layers correspond to the fully-connected classifier. Model was trained in the same manner as the DNN classifier described in the previous Subsection 2.1.1.

Interpretation of feature selection results for image recognition problem is not that straightforward in comparison to the simple perceptron classifier, as the convolution operations need input data to maintain well-defined

shape. It could be intuitively understood by the fact that it is impossible for human to choose some low number of points in the image which will be enough for identification. Instead, the BSF could provide an attention maps, i.e. to highlight the regions of images with highest information density for classification. The BSF layer was placed as input layer of the CNN classifier which was then trained at the above-described manner. After training, weights of the BSF layer contain information about feature importances.

2.1.3. Spectra recognition

The interpretation of complex compounds spectra is a known problem in analytical chemistry. Few reports on successful use of machine learning techniques for identification of the biological samples were published [27, 28]. The binary stochastic filter was proposed during work on the similar problem, the classification of DNA spectra. Such spectra are not readable by human due to presence of thousands of different vibration frequencies, resulting in the overcomplicated and noisy data. Spectra were classified by the CNN model consisting of 3 convolutional and 4 fully-connected layers with satisfactory results. Thereafter binary stochastic filter layer was added to the model input and training process was repeated. Weights of BSF layer in that case correspond to the spectral regions of interest. Weights of the layer were visualized (Fig. 2 (b)) and treated as a regions of interest of a spectra. Correspondence between them and expected vibrational frequencies of the DNA constituents [29] were observed. This method allows to obtain the information about chemical changes in a set of similar compounds or mixtures, spectra of which are indistinguishable by other methods.

2.2. Self-optimizing neural network

Sparse neural networks are believed to be more efficient than popular fully-connected systems due to enhanced generalization, faster convergence and higher performance [30]. An alternative way to sparsifying is neuron pruning, the removal of least important units from the network, which was demonstrated by Mozer and Smolensky [31]. The latter approach seems to be more beneficial from the performance point of view as removal of the single unit leads to the greater decrease of computational complexity, nevertheless the former became more frequent, being popularized by the above-mentioned work of Le Cun [30]. Furthermore, the analysis of units importance is less complex because of significantly lower number in comparison to weights. By placing binary stochastic filter between NN layers it is

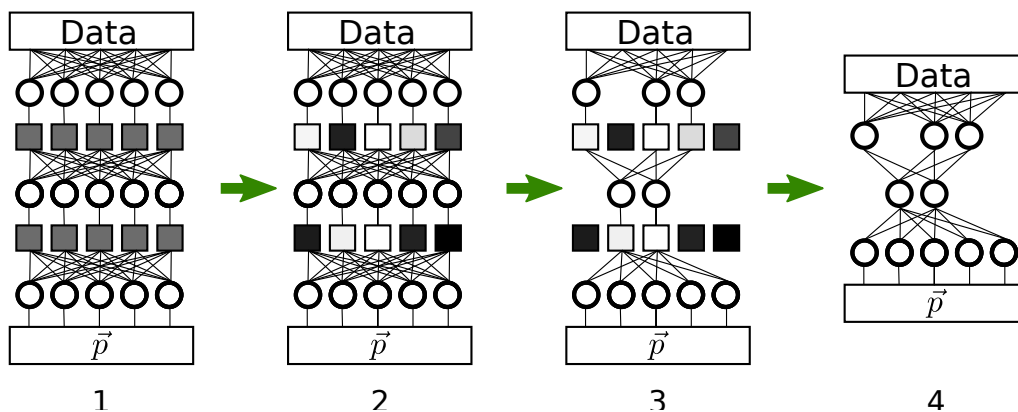


Fig. 3: Neuron pruning algorithm graphical summary

possible to disable the least important parts during training process. Applying the BSF unit to every interunit connection may be used to prune specific weights, while applying to the output of above-laying unit will cause neuron pruning. The second approach was selected according to above-described

reasons and straightforward implementation. The algorithm is schematically shown in the Figure 3.

1. The fully-connected model with excess units is built, and BSF units (drawn as squares) are placed after each dense layer.
2. During training process the weights of neurons and BSF are optimized (values of BSF units are visualized as lightness of the squares, i.e. dark values correspond to lower weights)
3. Weights of the filter are analyzed and neurons corresponding to the low weights are deleted.
4. The BSF layers are removed leaving the shape-optimized and trained NN model which could be additionally trained for fine-tuning.

The BSF layer was implemented in Keras framework with Tensorflow back-end [32, 33] based on above-discussed theory. All NN models used in experiments were built by dint of the same framework.

3. Results

Three different datasets were used, the *Wine* dataset [34], *KDD-99* [35] and *Musk2* dataset [36]. As an original KDD99 dataset is huge (around 5 millions of instances), a sample of around 1 million instances was used instead. The datasets summary is given in the Table 1. Datasets were standardized by removing mean and scaling to unit variance. Musk2 and KDD99 datasets contain categorical data labels which were encoded as integers before standardization.

Table 1: Classification datasets summary

	Instances	Classes	Features	Description
Wine	178	3	13	Chemical analysis of a wine from three different cultivars
KDD99	918455	21	41	Wide variety of intrusions data simulated in a military network environment.
Musk2	6598	2	168	Conformation of molecules judged to be musk or non-musk

3.1. Deep NN classifier

NN classifier was trained on each dataset and corresponding accuracies were saved as original. Feature selection was performed as it is described in the Subsection 2.1.1, and accuracy estimation was repeated for truncated versions of datasets. Obtained data is summarized in the Table 2 together with reference accuracies, found in literature. Additionally, the experiment was repeated for KDD99 dataset but with 12 least important features (corresponding BSF weights are below 30th percentile). Maximal accuracy has achieved 57.82 % in that case.

The implementation of silhouettes from the scikit-learn project [37] was used in the experiment. The method was applied to the original and truncated versions of *Wine* dataset. Obtained silhouettes coefficient (2.1.1) as a measure of cluster separation, was calculated as 0.2798 and 0.3785 respectively.

Stability of a binary filter was estimated by varying the structure of NN classifier, training the system with *KDD99* dataset and analyzing the

Table 2: Comparison of classification results for original and truncated versions of three given datasets (cross-validated)

	Wine	KDD99	Musk2
Training accuracy, original	1.000	0.9993	1.000
Testing accuracy, original	0.9891	0.9993	0.9066
Number of selected features	6	8	42
Training accuracy, truncated	1.000	0.9975	1.000
Testing accuracy, truncated	0.9889	0.9975	0.9251
Reference accuracy	0.9887 [38]	0.9941 [39]	0.8920 [36]

features of highest importance (above 80th percentile). Each experiment was repeated 4 times and selected features were summarized in the Table B.6. The column NN structure contains the number of units in each layer and their activation functions. Additionally, the output of every model consists of a softmax-activated layer, which is not shown in the table.

3.2. Convolutional Classifier

The MNIST dataset from the work of Le Cun et al. [24] was used for CNN training. The original set contains 60000 handwritten digit images of size 28x28 pixels with labels, from which 10000 were randomly sampled for the further experimenting. Implemented model structure is shown in the appendix (Table B.5). Model has achieved training and testing accuracies of 1.000 and 0.9865 respectively. BSF layer was added to model and training process was repeated. The weights of the layer were visualized (Fig. 2 (a)) and clearly correspond to the central part of image where most of

information about the digit is located. An animated demonstration of the training process could be found in the supplementary materials.

3.2.1. Spectra recognition

A classifier model was trained on spectra dataset, a sample of which is shown in the Fig. 2 (b). Weights of the layer are then visualized (Fig. 2 (c)) and treated as a regions of interest of a spectra.

3.3. Self-optimizing neural network

The experiment was performed with the datasets, used in the Section 2.1.1. It was found beneficial to normalize the L_1 penalty coefficient by number of units as it is applied separately to the BSF layers, which have different shape. The implementation utilizes additional functions for model rebuilding [40]. Model with excess neurons was trained on each dataset until convergence and then pruned. The weights of shape-optimized model were reseted and model was trained until convergence (number of epochs were determined experimentally to guarantee no loss decrease) in 10-fold cross-validation manner,

Mean values for accuracy are tabulated in the Table 3.

4. Discussion

4.1. Deep NN classifier

From the classification results (Table 2) one can conclude that correct feature selection may lead to significant increase of model performance without considerable loss of accuracy, as for each of three datasets the multifold dimensionality decrease was observed, leading to corresponding reduction

Table 3: Summary of the NN pruning results for different datasets and corresponding accuracies

	Wine	KDD99	Musk2
Training accuracy, original	1.000	0.9993	1.000
Testing accuracy, original	0.9891	0.9993	0.9066
Original number of units/weights	56/953	185/9430	666/138778
Number of units/weights after pruning	33/469	31/595	57/4103
Training accuracy, pruned	1.000	0.9993	1.000
Testing accuracy, original	0.9830	0.9993	0.9987

of computational complexity. Experiment with features corresponding to the lowest BSF weights proves that these features do not contain important information for classification problem.

Another important consequence is the fact that BSF allows to conclude which features in the dataset actually carry information. The importance distribution for two datasets (*Wine* and *KDD99*) is shown in the Appendix. It is possible to conclude that some of data, present in datasets is not meaningful in the classification problem, i.e. does not contain information about belonging to some class, like phenols concentration in Italian wine (Fig. B.6) or number of accessed files in the malware traffic (Fig. B.7). This could lead to interesting conclusions, like independence of phenols concentration on used cultivar. The *Musk2* dataset is not easily interpretable in the similar style, but the results could probably be even more important, as

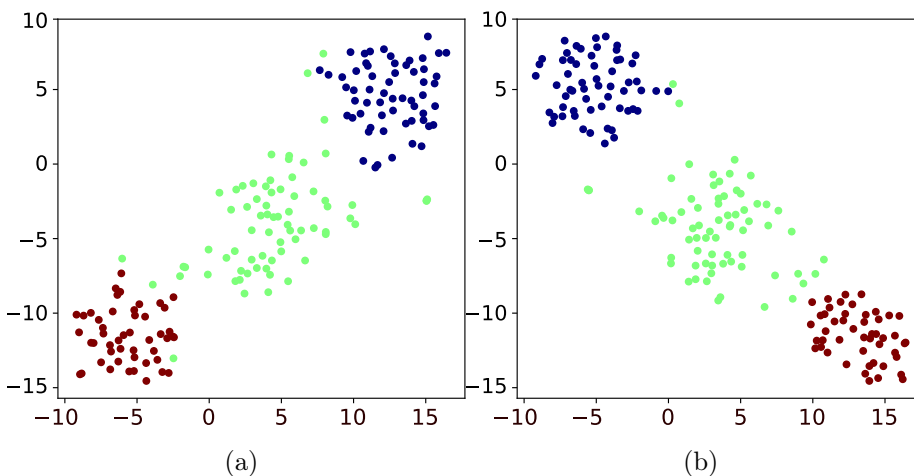


Fig. 4: Visual representation of the (a) original Wine dataset and (b) its truncated version, containing 6 most important features. It is visible that cluster separation has increased after removing unimportant features. Data was compressed down to 2 dimensions by T-SNE algorithm.

from the meaningful features the information about molecule biologically active sides could be extracted, which may be the valuable information for drug designers.

Thank to high popularity of KDD99 dataset it is possible to additionally compare feature selection results with results of other researchers, which are tabulated in the Table 4. In addition to 8 selected features, mentioned above, the truncated dataset was enlarged to 14 features, which is the minimal dimensionality leading to zero decrease of accuracy in comparison to original dataset. It is possible to conclude from the table, that BSF surpasses other feature selection methods in terms of accuracy per number of features. It is worth mentioning that in the works used for comparison, best testing accuracy was used as measure of classification success, while in the present work the cross-validated average accuracy is used.

Table 4: Comparison of feature selection results for KDD99 dataset

Method	Features	Accuracy	Reference
Fast correlation-based filtering, Naive Bayes/decision tree	12	0.9460	[41]
Decision tree, simulated annealing	28	0.9936	[42]
Support vector machine, particle swarm optimization	26	0.9945	[43]
Supported vector machine, simulated annealing	25	0.9942	[44]
Supported vector machine, decision tree, simulated annealing	23	0.9996	[42]
<i>Binary stochastic filtering</i>	<i>8</i>	<i>0.9975</i>	-
<i>Binary stochastic filtering</i>	<i>14</i>	<i>0.9993</i>	-

Values of silhouettes coefficient for the truncated Wine dataset were observed to be higher than for original version. Thus, removing unimportant features, that behave as noise, actually improves the dataset classification. Both versions were additionally processed with the well-known T-SNE algorithm [45], which allows high-dimensional data visualizing in the two-dimensional plot, which makes possible to see enhanced separation by naked eye. Generated images are shown in the Fig. 4

The stability estimating experiments demonstrate the fact that the BSF feature selector is relatively stable with only small portion of features chang-

ing in different experiments. It was found by manual observation of selected features importances, that differences in selections occurs from the threshold separation into important and unimportant. During selection, weights of some features are approaching unity, while another ones are approaching zero. Stochastic nature of selection process causes small deviations in the weights of most important features ($w \approx 1$), which lead to the fluctuations in selection results. This could be observed in the animation visualizing the BSF weights evolution during training process available in the supplementary materials.

4.1.1. Spectra recognition

Good correspondence between high-weight areas, threated as regions of interest and vibrational frequencies of the DNA constituents [29] was observed, which was expected from the chemical point of view. This method allows one to obtain the information about subtle chemical changes in difficult samples.

4.2. Self-optimizing neural network

Minimal decrease of accuracy was observed from the data, given in the Table 3, while number of weights was reduced significantly, from 2 to approximately 34 times. This corresponds to the enhance of performance for NN prediction of the same order, as computational complexity is directly connected to the number of weights. Such optimization could be especially beneficial for the embedded NN applications having limited computational resources. Obviously, the scale of NN pruning depends on initial redundancy but from the experiments it is possible to make empirical remark that satisfactory starting number of neurons in the hidden layers is equal

to the dimensionality of input data. Another important outcome is the fact that *Musk2* dataset, which was the most efficiently pruned, exhibits considerable increase of testing accuracy, i.e. improved generalization in correspondence with the [30]. Obtained cross-validated accuracy (0.9987) exceeds all experimental accuracies for the given dataset, found in literature (0.8920, 0.8333, 0.9600) [36, 46, 47].

5. Conclusion

Binary stochastic filter is highly straightforward method for estimating importances of input features or interneural connections. The method has a wide variety of possible applications, including feature selection and NN shape optimization. Thank to its layer structure it can be easily introduced to different kinds of NN without retraining. In experiments, method application allows selection of 8 features from 42 in the KDD99 dataset, bearing enough information for close-to-one prediction accuracy. Such kind of feature selection is of interest in natural sciences, as with its help one could make conclusions about processes, information of which is collected in the dataset. Suggested neuron pruning algorithm has lead to significant increase of NN performance in experiments, decreasing the number of weights in ≈ 34 times for Musk2 dataset. What even more substantial, after shape optimization 10-fold crossvalidation test demonstrated considerable increase of testing accuracy, proving better generalization. Thus, despite of its simplicity, the BSF approach is highly effective and could become a useful tool in the different fields of machine learning. Further work may include investigation of the weights pruning, i.e. network sparsifying and application of the method to more complex NN structures, such as adver-

serial networks or autoencoders.

References

- [1] M. L. Bermingham, R. Pong-Wong, A. Spiliopoulou, C. Hayward, I. Rudan, H. Campbell, A. F. Wright, J. F. Wilson, F. Agakov, P. Navarro, et al., Application of high-dimensional feature selection: evaluation for genomic prediction in man, *Scientific reports* 5 (2015) 10312. doi:doi:10.1038/srep10312.
- [2] T. Reuters, *Isi web of knowledge*, 2011.
- [3] F. Fleuret, Fast binary feature selection with conditional mutual information, *Journal of Machine Learning Research* 5 (2004) 1531–1555.
- [4] H. Peng, F. Long, C. Ding, Feature selection based on mutual information criteria of max-dependency, max-relevance, and min-redundancy, *IEEE Transactions on pattern analysis and machine intelligence* 27 (2005) 1226–1238. doi:doi:10.1109/tpami.2005.159.
- [5] L. Yu, H. Liu, Feature selection for high-dimensional data: A fast correlation-based filter solution, in: *Proceedings of the 20th international conference on machine learning (ICML-03)*, 2003, pp. 856–863.
- [6] K. Kira, L. A. Rendell, A practical approach to feature selection, in: *Machine Learning Proceedings 1992*, Elsevier, 1992, pp. 249–256.
- [7] M. Robnik-Šikonja, I. Kononenko, Theoretical and empirical analysis of relieff and rrelieff, *Machine learning* 53 (2003) 23–69.
- [8] H. Liu, R. Setiono, Chi2: Feature selection and discretization of numeric attributes, in: *Tools with artificial intelligence, 1995. proceedings., seventh international conference on*, IEEE, 1995, pp. 388–391.
- [9] Z. Zhao, H. Liu, Spectral feature selection for supervised and unsupervised learning, in: *Proceedings of the 24th international conference on Machine learning*, ACM, 2007, pp. 1151–1157.
- [10] S. Gu, R. Cheng, Y. Jin, Feature selection for high-dimensional classification using a competitive swarm optimizer, *Soft Computing* 22 (2018) 811–822.
- [11] M. Mafarja, I. Aljarah, A. A. Heidari, A. I. Hammouri, H. Faris, A.-Z. Ala’M, S. Mirjalili, Evolutionary population dynamics and grasshopper optimization approaches

- for feature selection problems, *Knowledge-Based Systems* 145 (2018) 25–45. doi:doi:10.1016/j.knosys.2017.12.037.
- [12] E. Hancer, B. Xue, M. Zhang, D. Karaboga, B. Akay, Pareto front feature selection based on artificial bee colony optimization, *Information Sciences* 422 (2018) 462–479. doi:doi:10.1016/j.ins.2017.09.028.
- [13] G. E. Hinton, T. J. Sejnowski, D. H. Ackley, Boltzmann machines: Constraint satisfaction networks that learn, Carnegie-Mellon University, Department of Computer Science Pittsburgh, PA, 1984.
- [14] H. Chen, S. Saïghi, L. Buhry, S. Renaud, Real-time simulation of biologically realistic stochastic neurons in vlsi, *IEEE transactions on neural networks* 21 (2010) 1511–1517. doi:doi:10.1109/tnn.2010.2049028.
- [15] M. Suri, D. Querlioz, O. Bichler, G. Palma, E. Vianello, D. Vuillaume, C. Gamrat, B. DeSalvo, Bio-inspired stochastic computing using binary cbram synapses, *IEEE Transactions on Electron Devices* 60 (2013) 2402–2409. doi:doi:10.1109/ted.2013.2263000.
- [16] N. Srivastava, G. Hinton, A. Krizhevsky, I. Sutskever, R. Salakhutdinov, Dropout: a simple way to prevent neural networks from overfitting, *The Journal of Machine Learning Research* 15 (2014) 1929–1958.
- [17] Y. Bengio, N. Léonard, A. Courville, Estimating or propagating gradients through stochastic neurons for conditional computation, *arXiv preprint arXiv:1308.3432* (2013).
- [18] G. Hinton, *Neural networks for machine learning*, 2012.
- [19] J. S. Bridle, Probabilistic interpretation of feedforward classification network outputs, with relationships to statistical pattern recognition, in: *Neurocomputing*, Springer, 1990, pp. 227–236.
- [20] C. Bishop, C. M. Bishop, et al., *Neural networks for pattern recognition*, Oxford university press, 1995.
- [21] V. Nair, G. E. Hinton, Rectified linear units improve restricted boltzmann machines, in: *Proceedings of the 27th international conference on machine learning (ICML-10)*, 2010, pp. 807–814.
- [22] D. P. Kingma, J. Ba, Adam: A method for stochastic optimization, *arXiv preprint*

- arXiv:1412.6980 (2014).
- [23] P. J. Rousseeuw, Silhouettes: a graphical aid to the interpretation and validation of cluster analysis, *Journal of computational and applied mathematics* 20 (1987) 53–65. doi:doi:10.1016/0377-0427(87)90125-7.
 - [24] Y. LeCun, B. E. Boser, J. S. Denker, D. Henderson, R. E. Howard, W. E. Hubbard, L. D. Jackel, Handwritten digit recognition with a back-propagation network, in: *Advances in neural information processing systems*, 1990, pp. 396–404.
 - [25] Y. LeCun, L. Bottou, Y. Bengio, P. Haffner, Gradient-based learning applied to document recognition, *Proceedings of the IEEE* 86 (1998) 2278–2324. doi:doi:10.1109/5.726791.
 - [26] S. Ioffe, C. Szegedy, Batch normalization: Accelerating deep network training by reducing internal covariate shift, *arXiv preprint arXiv:1502.03167* (2015).
 - [27] M. Gniadecka, P. A. Philipsen, S. Wessel, R. Gniadecki, H. C. Wulf, S. Sigurdsson, O. F. Nielsen, D. H. Christensen, J. Hercogova, K. Rossen, H. K. Thomsen, L. K. Hansen, Melanoma diagnosis by raman spectroscopy and neural networks: Structure alterations in proteins and lipids in intact cancer tissue, *Journal of Investigative Dermatology* 122 (2004) 443 – 449. doi:doi:10.1046/j.0022-202x.2004.22208.x.
 - [28] S. Sigurdsson, P. A. Philipsen, L. K. Hansen, J. Larsen, M. Gniadecka, H.-C. Wulf, Detection of skin cancer by classification of raman spectra, *IEEE transactions on biomedical engineering* 51 (2004) 1784–1793. doi:doi:10.1109/tbme.2004.831538.
 - [29] F. Madzharova, Z. Heiner, M. Guhlke, J. Kneipp, Surface-enhanced hyper-raman spectra of adenine, guanine, cytosine, thymine, and uracil, *The Journal of Physical Chemistry C* 120 (2016) 15415–15423. doi:doi:10.1021/acs.jpcc.6b02753.
 - [30] Y. LeCun, J. S. Denker, S. A. Solla, Optimal brain damage, in: *Advances in neural information processing systems*, 1990, pp. 598–605.
 - [31] M. C. Mozer, P. Smolensky, Skeletonization: A technique for trimming the fat from a network via relevance assessment, in: *Advances in neural information processing systems*, 1989, pp. 107–115.
 - [32] F. Chollet, et al., Keras, <https://keras.io>, 2015.
 - [33] M. Abadi, A. Agarwal, P. Barham, E. B. et al., TensorFlow: Large-scale machine learning on heterogeneous systems, 2015. URL: <https://www.tensorflow.org/>,

software available from tensorflow.org.

- [34] M. Forina, S. Aeberhard, R. Leardi, Wine dataset, PARVUS, Via Brigata Salerno, <https://archive.ics.uci.edu/ml/datasets/Wine> (2012).
- [35] S. Chaudhuri, D. Madigan, U. Fayyad, Kdd-99: The fifth acm sigkdd international conference on knowledge discovery and data mining, *SIGKDD Explor. Newsl.* 1 (2000) 49–51. doi:doi:10.1145/846183.846194.
- [36] T. G. Dietterich, R. H. Lathrop, T. Lozano-Pérez, Solving the multiple instance problem with axis-parallel rectangles, *Artificial intelligence* 89 (1997) 31–71. doi:doi:10.1016/s0004-3702(96)00034-3.
- [37] F. Pedregosa, G. Varoquaux, A. Gramfort, V. Michel, B. Thirion, O. Grisel, M. Blondel, P. Prettenhofer, R. Weiss, V. Dubourg, J. Vanderplas, A. Passos, D. Cournapeau, M. Brucher, M. Perrot, E. Duchesnay, Scikit-learn: Machine learning in Python, *Journal of Machine Learning Research* 12 (2011) 2825–2830.
- [38] B. Misra, S. Dehuri, Functional link artificial neural network for classification task in data mining, *Journal of Computer Science* (2007). doi:doi:10.3844/jcssp.2007.948.955.
- [39] A. K. Shrivias, A. K. Dewangan, An ensemble model for classification of attacks with feature selection based on kdd99 and nsl-kdd data set, *International Journal of Computer Applications* 99 (2014) 8–13. doi:doi:10.5120/17447-5392.
- [40] B. Whetton, Keras-surgeon, 2018. URL: <https://github.com/BenWhetton/keras-surgeon>.
- [41] D. H. Deshmukh, T. Ghorpade, P. Padiya, Improving classification using preprocessing and machine learning algorithms on nsl-kdd dataset, in: *Communication, Information & Computing Technology (ICCICT), 2015 International Conference on*, IEEE, 2015, pp. 1–6.
- [42] S.-W. Lin, K.-C. Ying, C.-Y. Lee, Z.-J. Lee, An intelligent algorithm with feature selection and decision rules applied to anomaly intrusion detection, *Applied Soft Computing* 12 (2012) 3285–3290. doi:doi:10.1016/j.asoc.2012.05.004.
- [43] S.-W. Lin, K.-C. Ying, S.-C. Chen, Z.-J. Lee, Particle swarm optimization for parameter determination and feature selection of support vector machines, *Expert systems with applications* 35 (2008) 1817–1824. doi:doi:10.1016/j.eswa.2007.08.088.

- [44] S.-W. Lin, Z.-J. Lee, S.-C. Chen, T.-Y. Tseng, Parameter determination of support vector machine and feature selection using simulated annealing approach, *Applied soft computing* 8 (2008) 1505–1512. doi:doi:10.1016/j.asoc.2007.10.012.
- [45] L. v. d. Maaten, G. Hinton, Visualizing data using t-sne, *Journal of machine learning research* 9 (2008) 2579–2605.
- [46] Q. Zhang, S. A. Goldman, Em-dd: An improved multiple-instance learning technique, in: *Advances in neural information processing systems*, 2002, pp. 1073–1080.
- [47] M.-L. Zhang, Z.-H. Zhou, Improve multi-instance neural networks through feature selection, *Neural Processing Letters* 19 (2004) 1–10.

Appendix A. Proof of gradients independence on introducing BSF layer

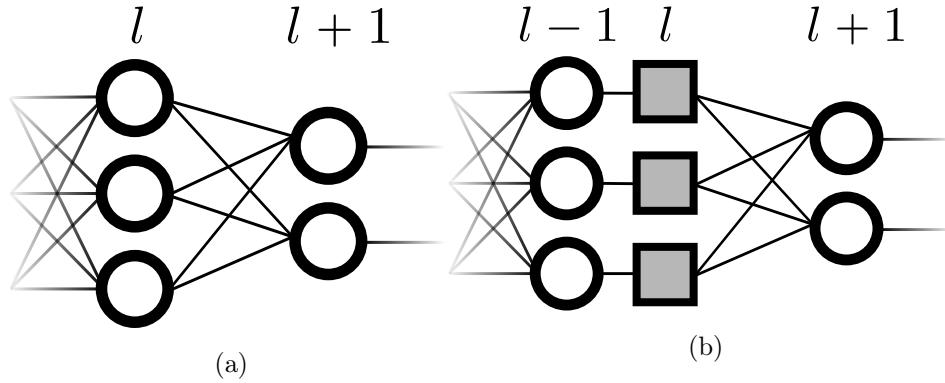


Fig. A.5

PROOF 1. Suppose the multilayer perceptron is given. Let us concentrate on the two hidden layers in the perceptron, having indices l and $l+1$ and containing i and j neurons in each respectively (Fig. A.5 (a)). Suppose the partial derivatives of loss function L with respect to the neuron pre-activation z_j^{l+1} is given. Let us call this value $\delta_j^{l+1} = \frac{\partial L}{\partial z_j^{l+1}}$ an error of the j neuron in the $l+1$ layer, which could be computed from the classical

backpropagation algorithm, and is enough for the computing of derivatives with respect to weights, as $\frac{\partial L}{\partial w_{ij}^{l+1}} = \frac{\partial L}{\partial z_j^{l+1}} \frac{\partial z_j^{l+1}}{\partial w_{ij}^{l+1}}$. Now the error of the neuron in l layer could be calculated using chain rule as

$$\delta_i^l = \sum_j \frac{\partial L}{\partial z_j^{l+1}} \frac{\partial z_j^{l+1}}{\partial a_i^l} \frac{\partial a_i^l}{\partial z_i^l} \quad (\text{A.1})$$

where a_i^l stands for activation (output) of the i neuron in l layer. $\frac{\partial z_j^{l+1}}{\partial a_i^l}$ could be derived from the equation describing neuron, $z_j^{l+1} = \sum_i a_i^l w_{ij}^{l+1} + b_j^{l+1}$ (w_{ij}^{l+1} corresponds to weight, connecting the i^{th} neuron from l with j^{th} neuron in $l+1$, b_j^{l+1} to corresponding neuron bias). As activation a_i^l is independent on other neurons in l layer, the sum could be omitted. By differentiating:

$$\frac{\partial z_j^{l+1}}{\partial a_i^l} = w_{ij}^{l+1} \quad (\text{A.2})$$

Last term $\frac{\partial a_i^l}{\partial z_i^l}$ could be derived at a similar manner, as $a_i^l = \text{act}(z_i^l)$, where $\text{act}(z)$ is activation function,

$$\frac{\partial a_i^l}{\partial z_i^l} = \text{act}'(z_i^l) \quad (\text{A.3})$$

Substituting A.2 and A.3 into A.1, the equation for computing error of the neurons in l layer could be obtained ($\text{act}'(z_i^l)$ is independent on indices of neurons in $l+1$ layer, so it could be factored out):

$$\delta_i^l = \text{act}'(z_i^l) \sum_j \delta_j^{l+1} w_{ij}^{l+1} \quad (\text{A.4})$$

Now suppose a BSF layer is introduced in between two classical layers, as it shown in the Fig. A.5 (b). Now numbering will be performed by indices i, j, k for every consequent layer. Then

$$\delta_i^{l-1} = \sum_k \frac{\partial L}{\partial z_k^{l+1}} \frac{\partial z_k^{l+1}}{\partial a_j^l} \frac{\partial a_j^l}{\partial z_j^l} \frac{\partial z_j^l}{\partial a_i^{l-1}} \frac{\partial a_i^{l-1}}{\partial z_i^{l-1}} \quad (\text{A.5})$$

Two members of this formula are known from previous derivation, $\frac{\partial a_j^l}{\partial z_j^l}$ which is a derivative of BSF unit with respect to its input is equal to 1 from the definition of ST estimator. $\frac{\partial z_j^l}{\partial a_i^{l-1}} = 1$, as BSF unit has only one input, thus $z_j^l = a_i^{l-1}$. Last term is similar to A.3. Substituting everything, factoring out independent on sum member, obtaining:

$$\delta_i^{l-1} = act'(z_i^{l-1}) \sum_k \delta_k^{l+1} w_{jk}^{l+1} \quad (\text{A.6})$$

By comparing this equation with A.4, one can conclude that BSF layer actually does not influence the backpropagation process by other way than filtering out some of the interneuron connections. This means that under $l1$ regularization constraints of BSF layer, NN will tend to find some minimal number of neurons, corresponding to the smallest loss function.

Appendix B.

Details about convolutional NN, used in the MNIST images classification (2.1.2) are given in the table B.5.

Highest importance features, selected by BSF method with different structure (3.1) of used NN is tabulated in the Table B.6. The diagrams demonstrating specific feature importances are given in the Figs. B.6 and B.7

Table B.5: Architecture of the convolutional NN classifier. Numerical parameters for convolution, max pooling and fully connected layers correspond to kernel size, pool size and number of neurons respectively.

Layer	Parameters	Activation
Convolution	3x3, 32 kernels	relu
Max pooling	2x2, batch normalization	-
Convolution	3x3, 48 kernels	relu
Max pooling	2x2, batch normalization	-
Convolution	3x3, 64 kernels	relu
Max pooling	2x2, batch normalization	-
Fully connected	1024	relu
Fully connected	100	relu
Fully connected	100	relu
Fully connected	10	softmax

Table B.6: Indices of selected features for different classifier structure

NN structure	Selected features
41, relu	[1, 2, 9, 22, 28, 34, 35, 36]
82, relu	[1, 3, 7, 9, 22, 34, 35, 36]
41, relu	[3, 7, 9, 22, 28, 34, 35, 36]
	[1, 7, 9, 22, 31, 34, 35, 36]
41, tanh	[3, 7, 9, 28, 31, 34, 35, 36]
41, relu	[7, 9, 22, 28, 31, 34, 35, 36]
41, relu	[1, 7, 9, 22, 28, 31, 34, 35]
41, relu	[7, 9, 22, 28, 31, 34, 35, 36]
41, tanh	[1, 7, 22, 28, 31, 34, 35, 36]
82, tanh	[3, 7, 9, 22, 31, 34, 35, 36]
41, tanh	[3, 7, 9, 22, 28, 34, 35, 36]
	[1, 7, 22, 28, 31, 34, 35, 36]
41, relu	[1, 7, 9, 22, 28, 34, 35, 36]
20, relu	[3, 7, 9, 22, 28, 34, 35, 36]
13, relu	[3, 7, 9, 22, 31, 34, 35, 36]
10, relu	[1, 7, 9, 22, 28, 34, 35, 36]
8, relu	

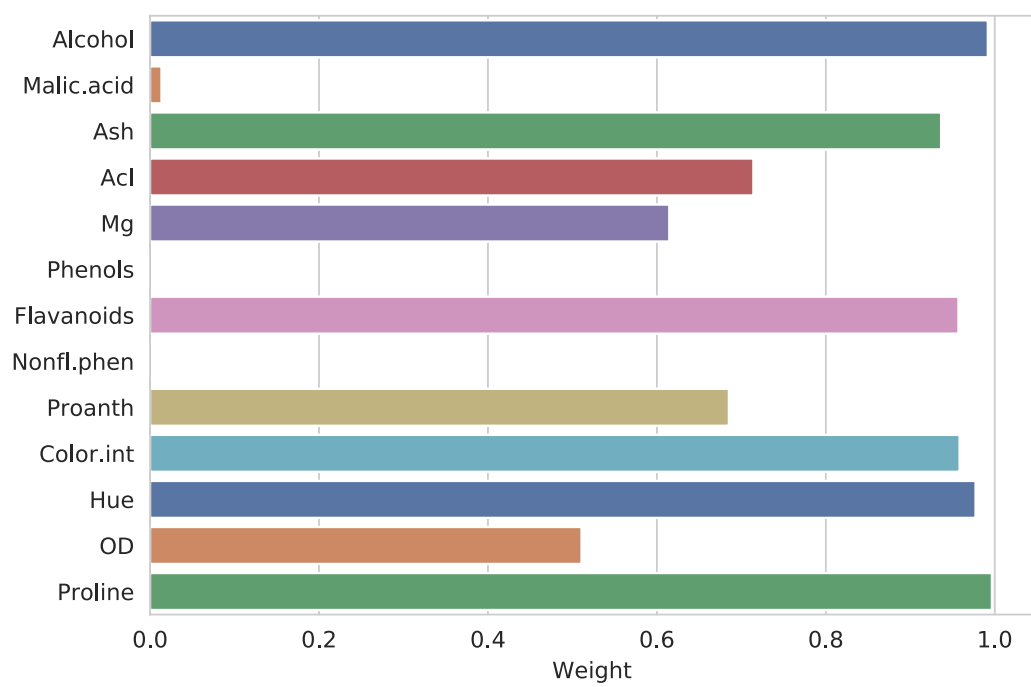


Fig. B.6: Feature importances distribution for the *Wine* dataset

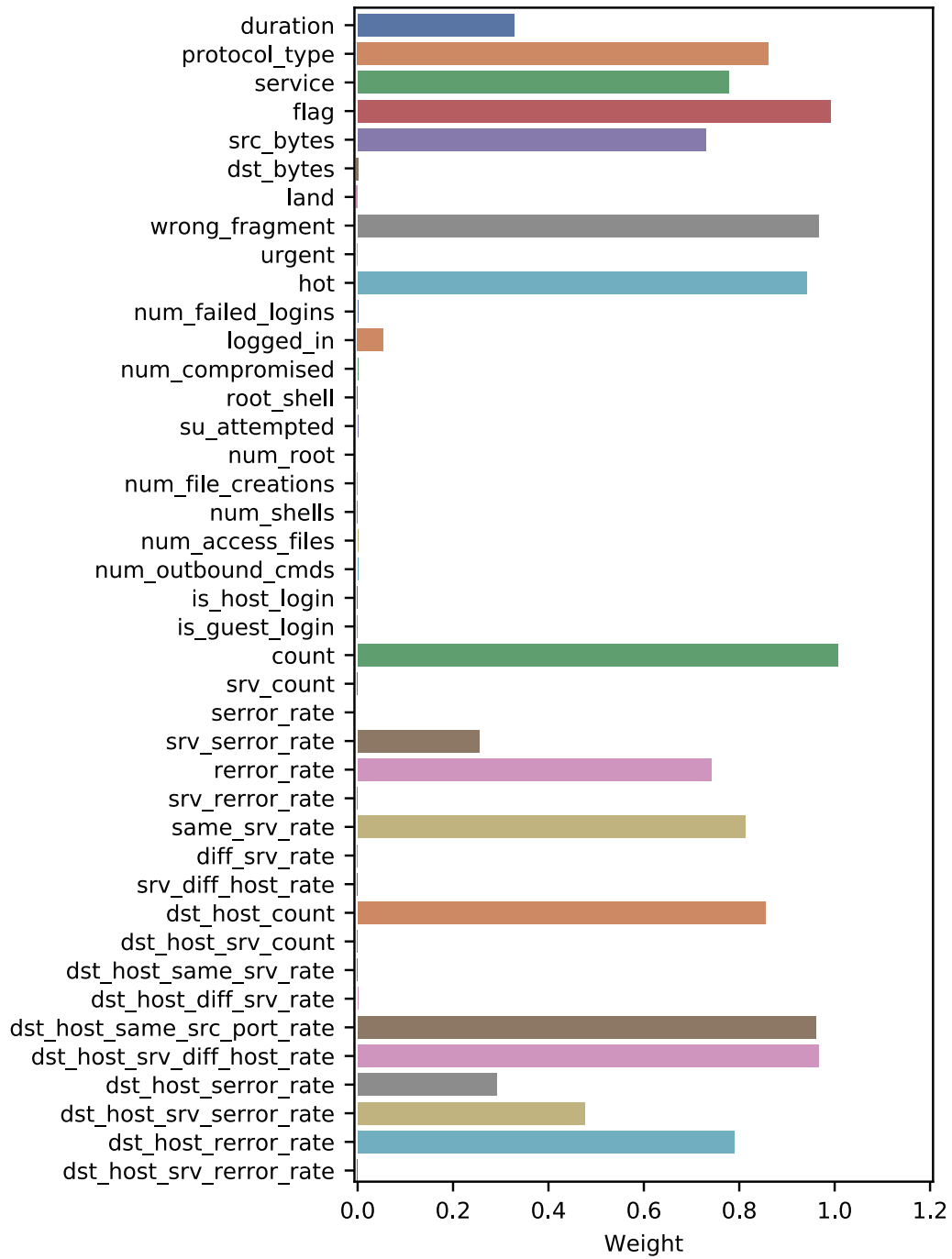


Fig. B.7: Feature importances distribution for KDD99 dataset